

## Research Article

Chenyu Yang, Hang Yu\*, Hui Xie, Shunfeng Peng, Jiangfei Tian, Zhiwu Gao, and Tian Luo

# Study on sedimentary model of Shanxi Formation – Lower Shihezi Formation in Da 17 well area of Daniudi gas field, Ordos Basin

<https://doi.org/10.1515/geo-2022-0752>

received September 13, 2024; accepted December 02, 2024

**Abstract:** The Daniudi gas field in the Ordos Basin is a significant area for developing tight sandstone gas reservoirs in China. This study focuses on the Permian Shanxi and Lower Shihezi formations in the Da 17 well area, analyzing sedimentary model through petrological characteristics, physical properties, pore characteristics, and lithofacies characteristics. Findings reveal that the Shanxi Formation belongs to the deltaic plain sedimentary environment, which is divided into distributary channel and inter-channel, and identifies the microfacies of the main distributary channel and the sub-distributary channel. The Lower Shihezi Formation exhibits braided channel sediments, dividing them into channel bar sediments and flood plain sediments, and identifying isolated channel microfacies and superimposed channel microfacies. Analysis shows that sedimentation has an impact on reservoir properties through particle size, lithological characteristics, and sedimentary microfacies. The main distributary channel and superimposed sandbars are favorable microfacies for the formation of gas reservoirs. The porosity of the main diversion channel ranges from 8 to 13%, and the permeability ranges from 0.3 to  $0.6 \times 10^{-3} \text{ m}^2$ . The porosity of the superimposed sandbar ranges from 8 to 15%, with a permeability of  $0.3\text{--}2.2 \times 10^{-3} \text{ m}^2$ . This study provides a theoretical foundation advancing tight sandstone gas development in the Daniudi gas field.

**Keywords:** Ordos Basin, Lower Paleozoic, tight sandstone, sedimentary microfacies, reservoir properties

## 1 Introduction

By the end of 2022, cumulative proven geological oil reserves in China reached 10.52 billion tones, while natural gas reserves totaled 6.86 trillion cubic meters [1]. Tight sandstone gas is one of the important types of unconventional oil and gas resources. Numerous successful examples of commercial tight gas exploration highly have relied on the discovery of high-quality sandstone reservoirs [1,2]. Sedimentary facies, sequence and architecture of sandstone, and diagenetic alterations significantly control reservoir quality. Among these, sedimentary facies are closely linked to sediment characteristics, including mineral composition, grain size, and initial water properties [3–10]. Thus, analyzing the sedimentary model and evolution of tight sandstone, and discussing the influence of sedimentary conditions and lithology on reservoirs is essential for a deeper understanding of the formation and storage potential of tight sandstone reservoirs [11–18].

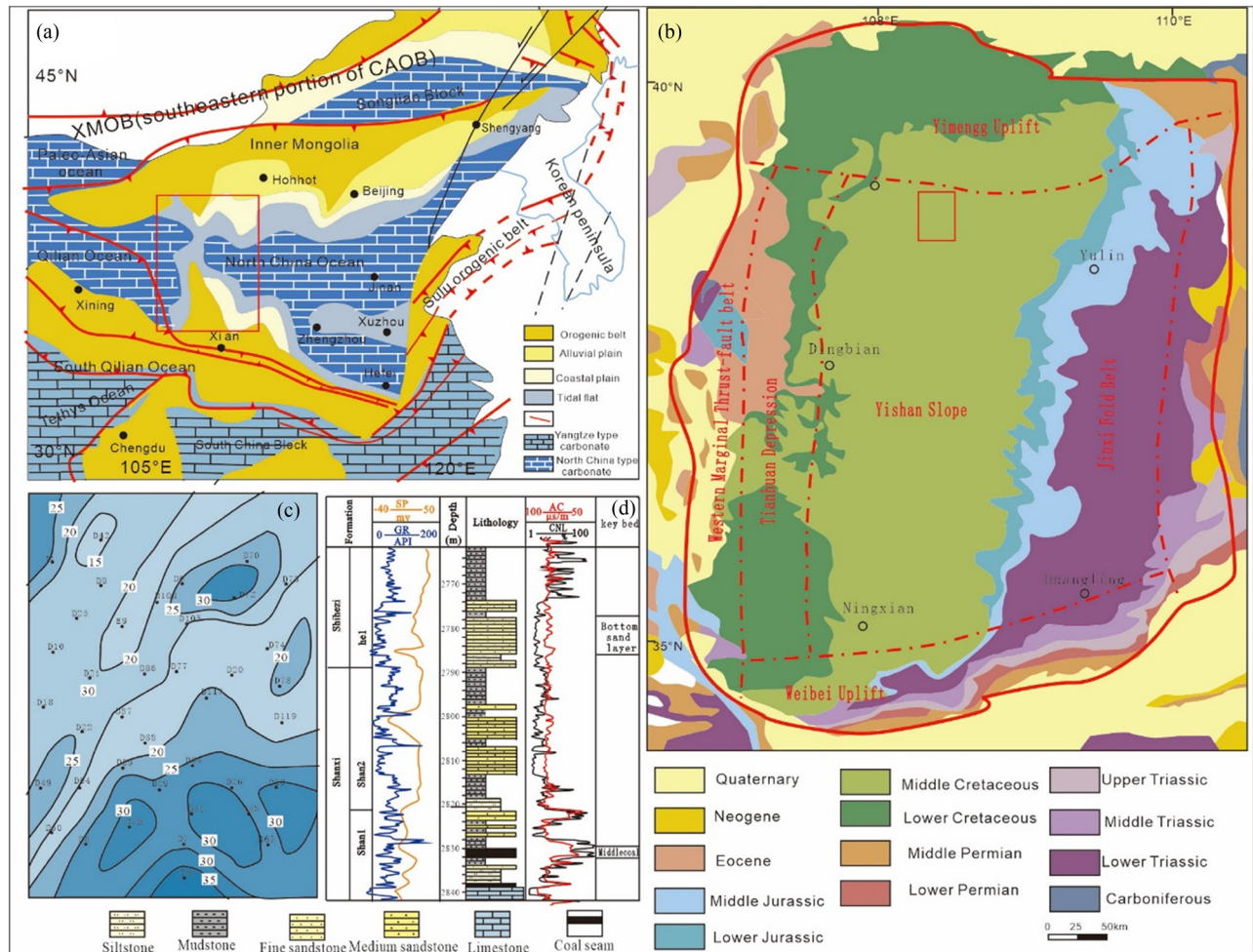
The Ordos Basin, located in the North China Plate (Figure 1a), is a major oil and gas basin in western China, with particularly rich oil and gas resources in tight sandstones [19–25]. In recent years, multiple gas-bearing series have been discovered in the Paleozoic strata of the Daniudi gas field in the northern Ordos Basin, leading to the formation of substantial lithologic reservoirs in river channels, distributary channels, and sand bars. These oil and gas reservoirs are characterized by low porosity, low permeability, and low abundance [26–32]. The coal-bearing tight sandstone strata developed in a marine-continental transition environment and represented by the Permian Shanxi Formation – Lower Shihezi Formation, have achieved significant breakthroughs, particularly with the 1HF well. In the past, scholars have conducted a lot of research on the formation and distribution of tight sandstones in the Shanxi

\* **Corresponding author: Hang Yu**, Sichuan Institute of Comprehensive Geological Survey, Chengdu, 610084, China, e-mail: 463792633@qq.com  
**Chenyu Yang, Zhiwu Gao, Tian Luo:** Engineering College, Zunyi Normal University, Zunyi, 563000, China

**Hui Xie:** School of Intelligent Construction, Luzhou Vocational and Technical College, Luzhou, 646000, China

**Shunfeng Peng:** Evaluation and Utilization of strategic Rare Metals and Rare Earth Resource Key Laboratory of Sichuan Province, Sichuan Experimental Testing Research Center of Natural Resources, Chengdu, 610081, China

**Jiangfei Tian:** Sichuan Geophysical Survey and Research Institute, Chengdu, 610000, China



**Figure 1:** (a) Regional structural map of the Ordos Basin. (b) Structural location of Daniudi gas field. (c) Contour thickness map of the Lower Shihezi Formation in the Daniudi well area. (d) Comprehensive stratigraphic column chart of Shanxi Formation and Lower Shihezi Formation first member in the study area.

and Lower Shihezi Formations, but the genetic analysis of sedimentary sand bodies remains insufficiently detailed [33–37]. As a river type with high sand content [38], braided rivers play a crucial role in oil and gas enrichment. Scholars have conducted systematic studies on the depositional processes of braided rivers using braided river modeling [39–41], flume experiments [42,43], and computer simulations [44], especially the fine identification of the mechanism and type of the channel bar sedimentary microfacies [45–47]. However, research on channel bar sedimentary microfacies in the study area is still insufficient [45,48–51], especially for the microfacies delineation in braided river and braided river delta depositional environments is not precise enough, and there is still a need to further differentiate the sedimentary microphases of different types of channel bar and diversion channels. This article takes the Da 17 well area of the Daniudi gas field as an example, analyzing the sedimentary processes in the first member of the Lower Shihezi Formation and the Shanxi Formation, and focuses on the formation of

different types of channel bars and distributary channels, providing a basis for the understanding of the formation and distribution of tight sandstone, enriching the theory of tight sandstone gas accumulation in the Ordos Basin, and contributing a feasible means for the realization of the strategic goal of “stabilizing oil and increasing gas” in the oilfield.

## 2 Geological setting

The Ordos Basin covers an area of about 370,000 km<sup>2</sup>, located in the western part of the North China Craton, is a typical multi-rotational superposition basin [52]. According to the characteristics of stratigraphic development and the tectonic morphology of the basal top surface, it can be divided into tectonic units such as the western marginal thrust belt, the Yishan slope, the Jinxi flexural fold belt,

the Weibei uplift, and the Yimeng uplift [52,53]. The present Ordos Basin is a tectonic basin composed of a large syncline, which is deep in the west and shallow in the east, low in the south and high in the north.

The Daniudi gas field is located in the basin's north-eastern region, tectonically part of the Yishan slope (Figure 1b). The whole field is a gentle monocline, dipping to the southwest at less than  $1^\circ$ , with higher elevations in the northeast. The average thickness of the formation exposed by drilling wells is 3,000 m. The Da 17 well area is located in the southeast of the Daniudi gas field, with an area of 226 km<sup>2</sup>. Multiple gas reservoirs are developed in the Carboniferous Taiyuan Formation and the Permian Shanxi Formation, exemplifying the “three lows” of tight sandstone gas reservoirs: low pressure, low permeability, and low abundance [52–54]. Large-scale development of the gas field began in 2005, and more than 1,700 gas wells have been put into production, with cumulative output reaching 7.88 billion m<sup>3</sup>. This study focuses on the Permian Shanxi Formation and the first member of the Lower Shihezi Formation. The Shanxi Formation is a set of coal-bearing strata [55], mainly deposited in the delta plain. It can be divided into Shanxi Formation first and second member according to the lithological combination. The first member of the Lower Shihezi Formation is mainly braided river deposits, which is characterized by a large number of conglomerates. The lower coal seam of the Shanxi Formation and the sand layer at the bottom of the Lower Shihezi Formation are used as stratigraphic markers (Figure 1c), which can be well used for regional stratigraphic division and comparison (Figure 1d). The lower coal seam of the Shanxi Formation is located in the middle of the first member of the Shanxi Formation, with a thickness of 3–12 m, often sandwiched with carbonaceous mudstone. The corresponding logging curve is characterized by low gamma, low density, high resistance, high acoustic wave, and high neutron (showing the characteristics of “two lows and three highs”). The sand layer at the bottom of the Lower Shihezi Formation is the bottom boundary of the Shihezi first member, with the lithology of light gray gravelly coarse sandstone and medium coarse sandstone, with a thickness of 15–32 m [40,55], which is in contact with the underlying mudstone mutation. The logging curve is characterized by low gamma and negative natural potential anomaly, presenting a clear lithologic contrast on the stratigraphic profile.

### 3 Sampling and methods

This study selected 30 key wells in the Shanxi Formation – Lower Shihezi Formation of the Da 17 well area of the Daniudi

gas field, Ordos Basin, for observation, description, and analysis.

#### 3.1 Lithofacies analysis

Based on the analysis of rock structure, lithological characteristics, sedimentary structure, and sedimentary environment, nine lithofacies types were identified and their formation mechanisms analyzed.

#### 3.2 Thin section analysis

A total of 120 rock samples were prepared as 0.03 mm-thick slices. The pores were filled with red and blue epoxy resin to facilitate observation of pore characteristics. The instrument was a Nikon Eclipse LV100N POL polarizing microscope.

#### 3.3 X-ray diffraction analysis

Twenty-six core samples were analyzed to determine their mineral composition using a DX-2700 X-ray diffractometer at the State Key Laboratory of Reservoir Geology and Development Engineering (Chengdu University of Technology), following the JY/009-1996 standard.

#### 3.4 Porosity and permeability testing

A total of 246 samples were selected and made into cylinders (2.5 cm in diameter, 5 cm in length), and the porosity and permeability test characteristics of the cover layer were tested by physical methods. AutoPore V mercury porosimeter was used for mercury porosity determination.

#### 3.5 Scanning electron microscopy (SEM)

Eleven core samples were selected and analyzed by the Quanta250 FEG SEM to identify the morphology of minerals and pores, located at the State Key Laboratory of Oil and Gas Reservoir Geology and Exploitation, Chengdu University of Technology.



## 4 Results

### 4.1 Petrology characteristics

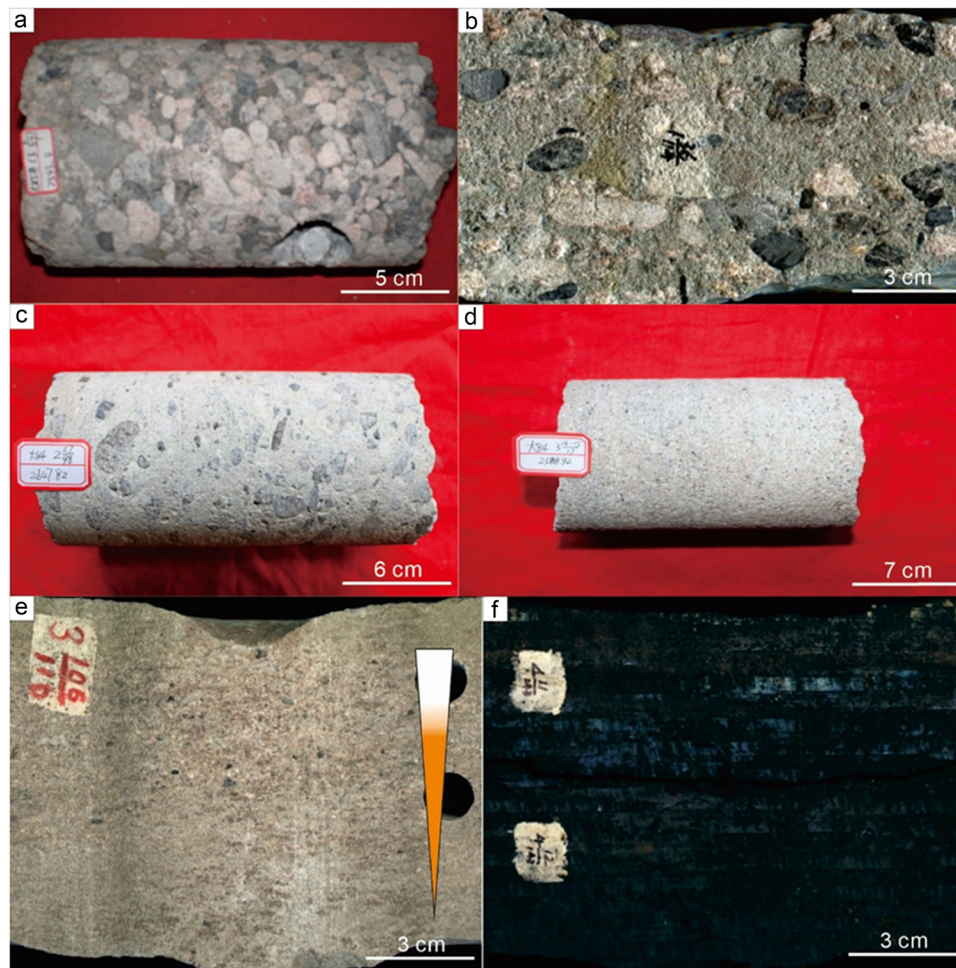
#### 4.1.1 Macropetrological characteristics

The Shanxi Formation and first member of the Lower Shihezi Formation in the study area are mainly terrigenous clastic rock deposits. The Shanxi Formation is mostly dark-colored mudstone, showing rich organic matter content, and the sandstone is mainly gray. It reflects that the climate is humid and the sedimentary environment is a weak reduction-reductive. In the first member of the Lower Shihezi Formation, the climatic characteristics show a gradual aridity, and the sandstone color lithology changes to brown and yellow. The rock types include conglomerate (Figure 2a),

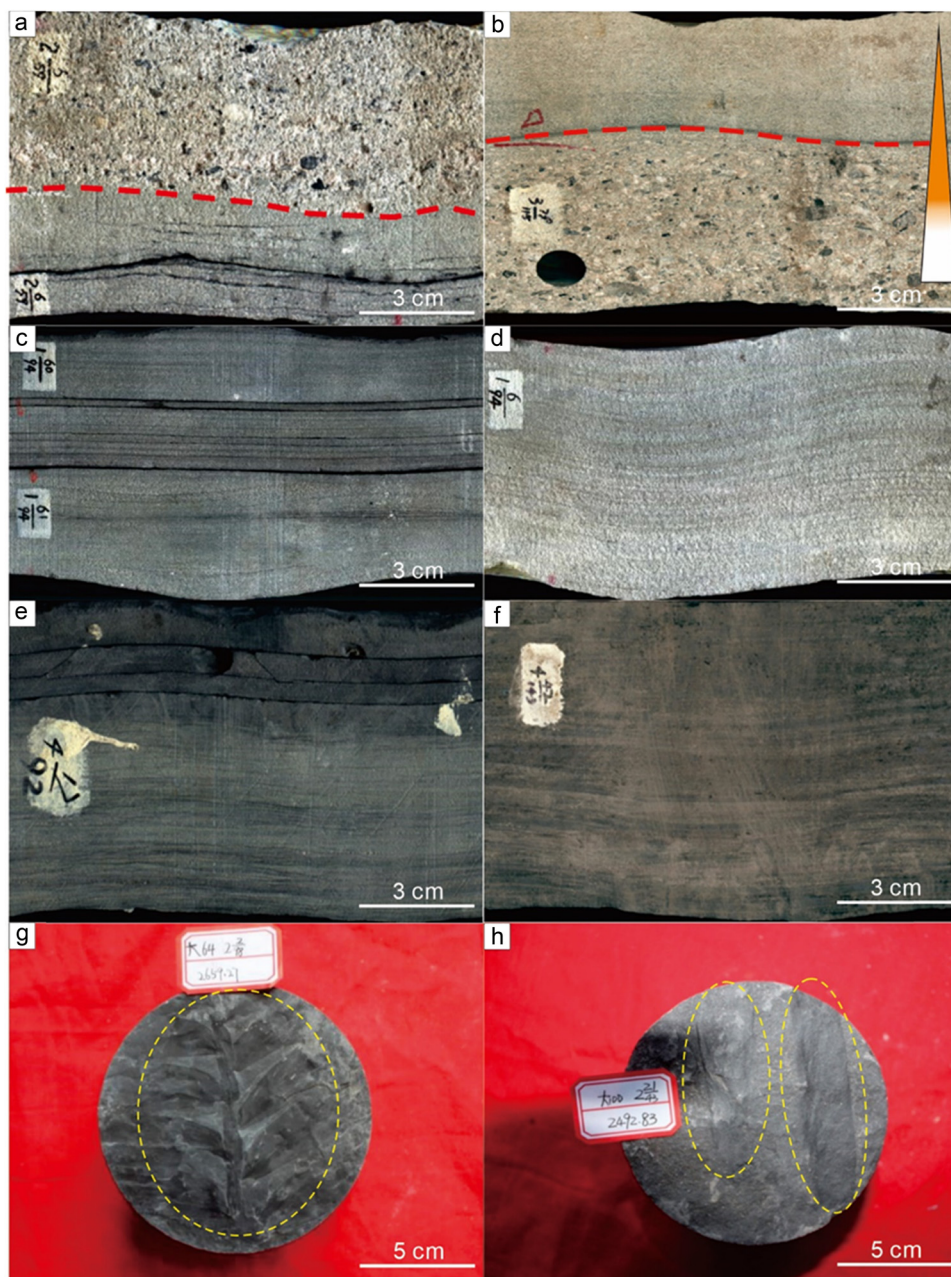
conglomerate-grained coarse sandstone (Figure 2b and c), coarse sandstone (Figure 2d and e), medium-fine sandstone, mudstone, and coal seam (Figure 2f). Typical sedimentary structures include scour surface, grain sequence bedding, parallel bedding, plate bedding, sand grain bedding, lenticular bedding, plant fossils, plant fragments, etc. (Figure 3).

#### 4.1.2 Rock and mineral characteristics

In the study area, 265 samples were selected for whole rock analysis. The lithology of the first member of the Lower Shihezi Formation is mainly lithic quartz sandstone and lithic sandstone, and very few samples are feldspar lithic sandstone (Figure 4). In contrast, the Shanxi Formation consists mainly of lithic quartz sandstone, lithic sandstone,



**Figure 2:** Rock characteristics of the Shanxi Formation and the Lower Shihezi Formation first member in the study area. (a) Conglomerate, Da 85 well, Lower Shihezi Formation first member, 2543.5 m. (b) Middle conglomerate, Da 70 well, Lower Shihezi Formation first member 1, 2543.5 m. (c) Gravelly coarse sandstone, Da 64 well, Lower Shihezi Formation first member, 2647.82 m. (d) Coarse sandstone, Da 84 well, Shanxi Formation, 2588.92 m. (e) Coarse sandstone, Da 20 well, Shanxi Formation, 2709.60 m. (f) Coal, Da 42 well, Shanxi Formation, 2560.30 m.

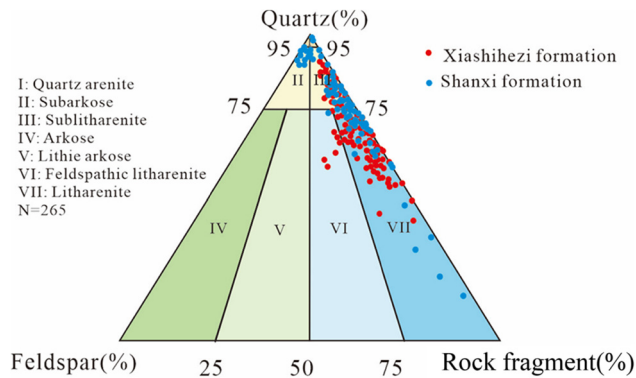


**Figure 3:** Sedimentary structure characteristics of Shanxi Formation and Lower Shihezi Formation first member in the study area. (a) Scouring surface, Da 49 well, Shanxi Formation, 2-59-05-06. (b) Positive grain sequence, Da 42 well, Shanxi Formation, 3-115-79. (c) Parallel bedding, Da 49 well, Lower Shihezi Formation first member, 1-94-60-61. (d) Plate oblique bedding, Da 49 well, Lower Shihezi Formation first member, 1-94-06. (e) Sand grain bedding, Da 26 well, Lower Shihezi Formation first member, 4-92-17. (f) Lenticular bedding, Da 42 well, Shanxi Formation, 4-143-42. (g) Fossil plants, Da 64 well, Shanxi Formation, 2659.27 m. (h) Plant stem fragments, Da 100 well, Shanxi Formation, 2492.83 m.

quartz sandstone, and a small amount of feldspar lithic sandstone. Compared to the first member of the Shihezi Formation, the Shanxi Formation is generally less clastic and richer in quartz content. The detritus in the Shanxi Formation is dominated by metamorphic quartz, phyllite, and kaolinite (Figure 5). The sorting of debris is medium deviation, the roundness is general, and the main shape is sub-angular. The debris particles

are mainly phyllite and metamorphic quartz, with occasional mica. Due to compaction, the banded mica is generally bent. The detritus in the Lower Shihezi first member exhibit poor to moderate sorting, with average particle roundness and mostly sub-angular. The reservoir rock interstitial material content ranges from 6 to 28%, mainly including kaolinite, illite, chlorite, authigenic clay film, calcite, and siliceous.





**Figure 4:** Ternary map of clastic rock content in the study area (ternary diagram based on the studies of Folk [56]).

## 4.2 Reservoir physical properties

### 4.2.1 Pore space characterization

The primary pore types in the study area are intergranular dissolved pores, intragranular dissolved pores, and micro-cracks (Figure 6). Intergranular dissolved pores are the most important pore type in the study area. Chlorite, quartz secondary enlargement and clay minerals can fill primary pores. Generally, the pores formed by chlorite and quartz secondary enlargement usually exceed 0.01 mm, and the pores filled by clay minerals are under 0.01 mm. The pores formed by dissolution of the interstitial material during diagenetic evolution are called secondary intergranular pores. Secondary intergranular pores formed by dissolution of iron – argillaceous matrix and argillaceous matrix can be seen in the study area. Intragranular dissolved pores develop within the grains (containing heavy minerals) after being dissolved to varying degrees and are called intragranular dissolution pores. These can be classified as follows: (i) dissolved pores in feldspar grains; (ii) intragranular dissolved pores of rock debris; (iii) flaky intragranular pores: refers to the mica fragments or mica flakes and the mica flakes is formed by dissolution, the pore morphology is often leaf-like, parallel to the mica cleavage seams; and (iv) intragranular micropores: micropores between clay minerals formed within particles after the aluminosilicate rock fragments in sandstone are altered into kaolinite and montmorillonite.

### 4.2.2 Porosity and permeability

#### 4.2.2.1 Physical characteristics of Shanxi Formation

The analysis of porosity and permeability of the Shanxi Formation in the study area (Figure 7) shows that the porosity distribution ranges from 0.1 to 13.9%, the average

porosity is 6%, and the peak value is 5–7%. The samples with porosity greater than 7% account for 54% of the total samples. The permeability distribution range is  $0.001\text{--}10.1 \times 10^{-3} \mu\text{m}^2$ , the average permeability is  $0.262 \times 10^{-3} \mu\text{m}^2$ , showing an obvious unimodal distribution with a peak value of  $0.1\text{--}1 \times 10^{-3} \mu\text{m}^2$ , accounting for 61% of the total sample.

#### 4.2.2.2 Physical characteristics of section first of Lower Shihezi Formation

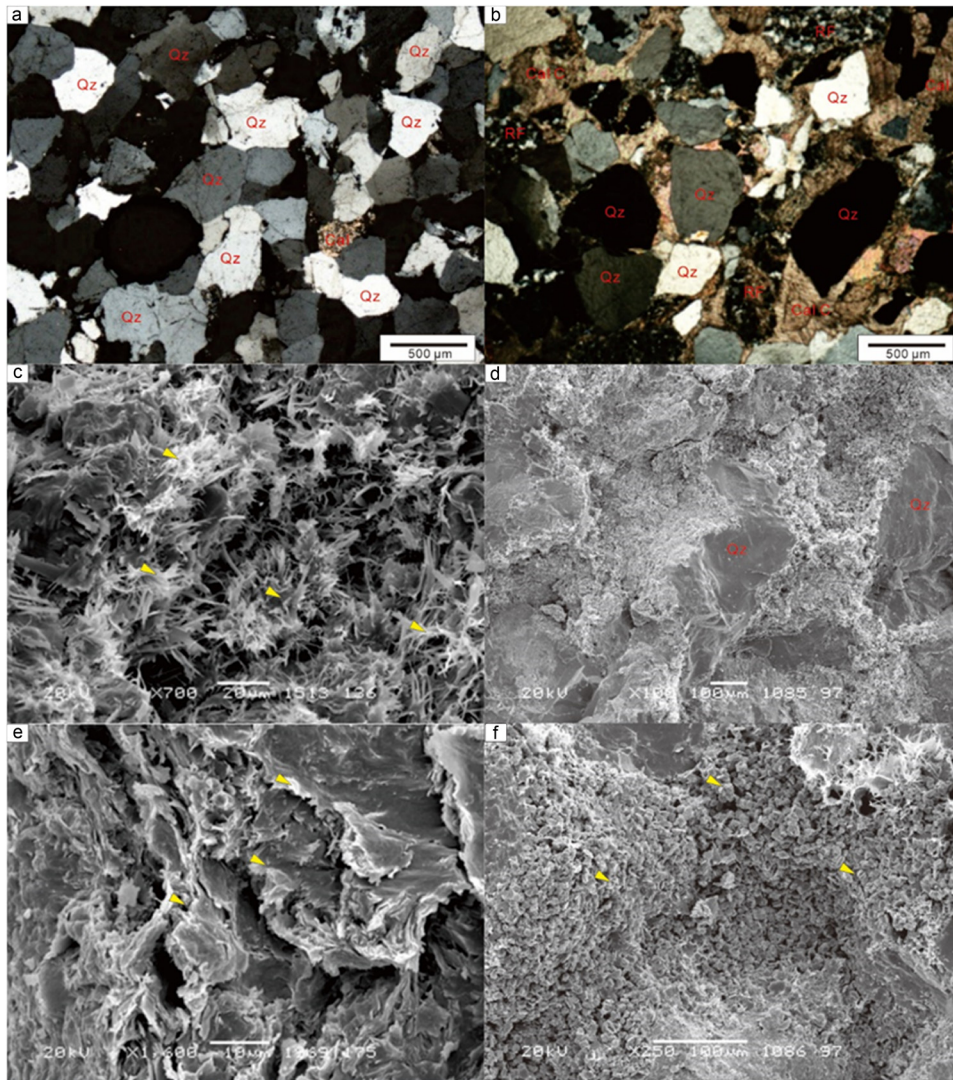
The analysis of porosity and permeability of first member of Lower Shihezi Formation in the study area shows that the porosity distribution range from 0.2 to 15.4%, the average porosity is 7.28%, and the peak value is 7–9%, of which the samples with a porosity greater than 7% account for 53% of the total number of samples (Figure 8). The permeability ranged from 0.001 to  $9.21 \times 10^{-3} \mu\text{m}^2$ , and the average permeability was  $0.86 \times 10^{-3} \mu\text{m}^2$ , showing an obvious single-peak distribution, with peaks in the range of  $0.1\text{--}1 \times 10^{-3} \mu\text{m}^2$ , accounting for 68% of the total number of samples.

## 4.3 Sedimentary systems

### 4.3.1 Types and characteristics of lithofacies

Based on core observation, ten lithofacies types were identified by lithology, sedimentary structure, and environment (Figure 9 and Table 1).

1. Massive bedding conglomerate facies: thick and massive, the gravel content is greater than 30%, the gravel is well rounded, and the gravel diameter is 3–6 cm, which belongs to the retention deposit at the bottom of the river.
2. Gravel-bearing coarse sandstone facies: the rock strata are middle-thick layers, mainly coarse sandstone, containing a small amount of gravel, with a content of less than 10%. It is a delta distributary channel deposit with strong hydrodynamic conditions, usually developed in the middle and lower parts of the channel.
3. Trough cross-bedding sandstone facies: the rock strata are dominated by medium-layered medium sandstone and a small amount of coarse sandstone. It is a typical channel filling deposit and developed in the middle and lower parts of the channel.
4. Tabular cross-bedding sandstone facies: the rock strata are mainly thin-bedded fine sandstone, with a small amount of medium sandstone, which is a typical under-water-classified river channel deposit.
5. Parallel bedding sandstone facies: the rock stratum is dominated by thin-layered fine sandstone, with a small



**Figure 5:** Microscopic characteristics of clastic rock content reservoir in the study area. (a) Quartz sandstone, Da 70 well, Shanxi Formation, 2433.19 m. (b) Lithic quartz sandstone, calcareous cementation development, Da 70 well, Shanxi formation, 2433.19 m. (c) Filamentous and hairy illites filled in intergranular pores, Da 77 well, Lower Shihezi Formation first member, 2526.97 m. (d) The rock structure is loose, and the kaolinite aggregate and filamentous illite are filled in the intergranular pores and between grains Da 70 well, Lower Shihezi Formation first member, 2374.53 m. (e) Sheet mica dissolution, alteration Da 83 well, Shanxi Formation, 2506.42 m. (f) Booklet-like kaolinite aggregates filled in intergranular pores, intergranular pores developed, Da 70 well, Lower Shihezi Formation first member, 2374.53 m.

amount of medium sandstone, which is a river sedimentary product under strong hydrodynamic conditions.

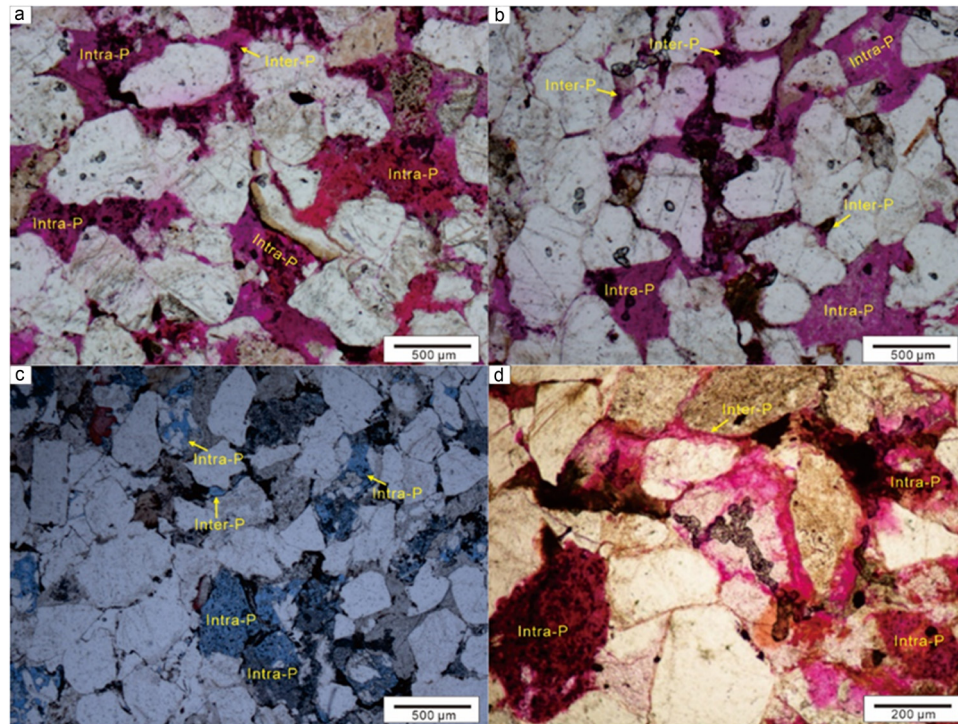
6. Deformed stratified sandstone facies: the rock layer is dominated by thin-bedded fine sandstone, siltstone, and a small amount of mudstone, which is the product of rapid sedimentation.
7. Wave bedding sandstone facies: the strata are mainly thin-bedded fine sandstone, siltstone, and a small amount of mudstone.
8. Sand grained bedding siltstone facies: the rock stratum is dominated by thin-bedded fine sandstone, siltstone, and a small amount of mudstone.

9. Horizontal bedding siltstone facies: the rock layers are composed of thin siltstone and mudstone, formed in a weak hydrodynamic environment, and is the main sedimentary product in the inter-distributary depression and inter-classified bays.
10. Dark mudstone facies: mainly former delta mud deposits, rich in organic matter.

#### 4.3.2 Types of sedimentary facies

In the study area, the sedimentary facies of the first member of the Lower Shihezi Formation primarily consist





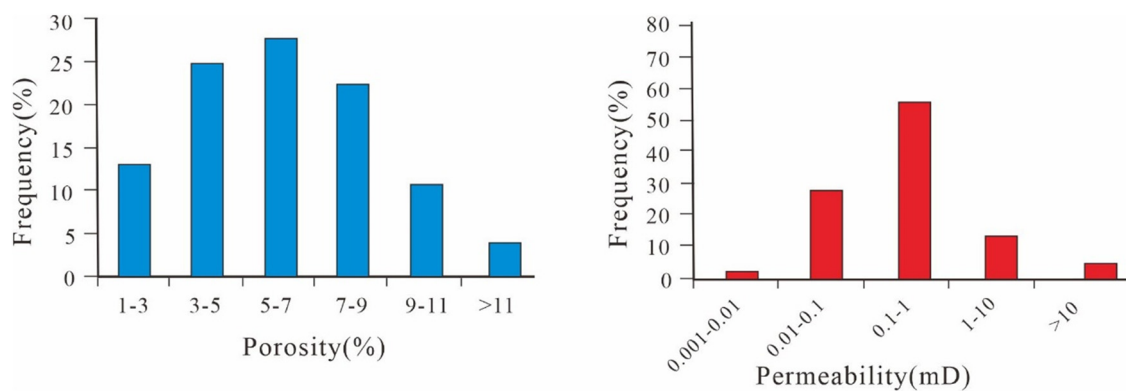
**Figure 6:** Characteristics of pore development in clastic rocks in the study area. (a) Intergranular dissolved pore and intergranular dissolved pore development, coarse lithic quartz sandstone, Da 70 well, 2490.18 m, Shanxi Formation,  $4 \times 10$  (-). (b) Intergranular dissolved pore and intergranular dissolved pore development, coarse lithic quartz sandstone, Da 71 well, Shanxi formation 2480.18 m,  $4 \times 10$  (-). (c) Intra-granular dissolved pores and a small amount of intergranular dissolved pores are developed, and lithic quartz sandstone, Da 107 well, 2357.17 m, Lower Shihezi Formation first member,  $10 \times 4$  (-). (d). Development characteristics of dissolution fractures, intra-granular and intergranular dissolution pores, fine-grained lithic sandstone, Da 56 well, Shanxi Formation, 2679.91 m,  $10 \times 10$  (-). Intra-P: intra-granular dissolved pore; Inter- P: intergranular pore.

of braided channel deposits, with further subdivision into channel bars and flood plains. In contrast, the Shanxi Formation is composed mainly of braided channel deltaic plain deposits, with distinct diverging channels and inter-channel deposits identified within these environments.

#### 4.3.2.1 Braided channel

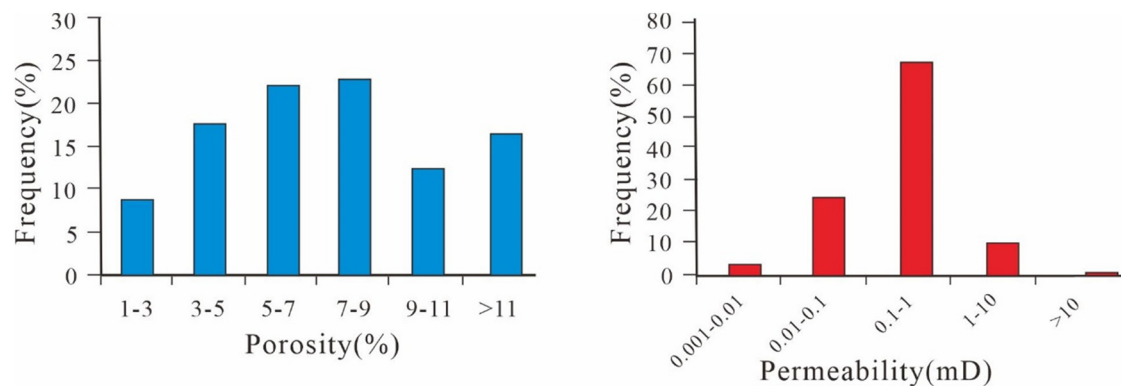
##### 4.3.2.1.1 Channel bar

Channel bars represent the most typical sedimentary feature in braided river channels, formed under strong hydrodynamic conditions. In addition, under the influence of

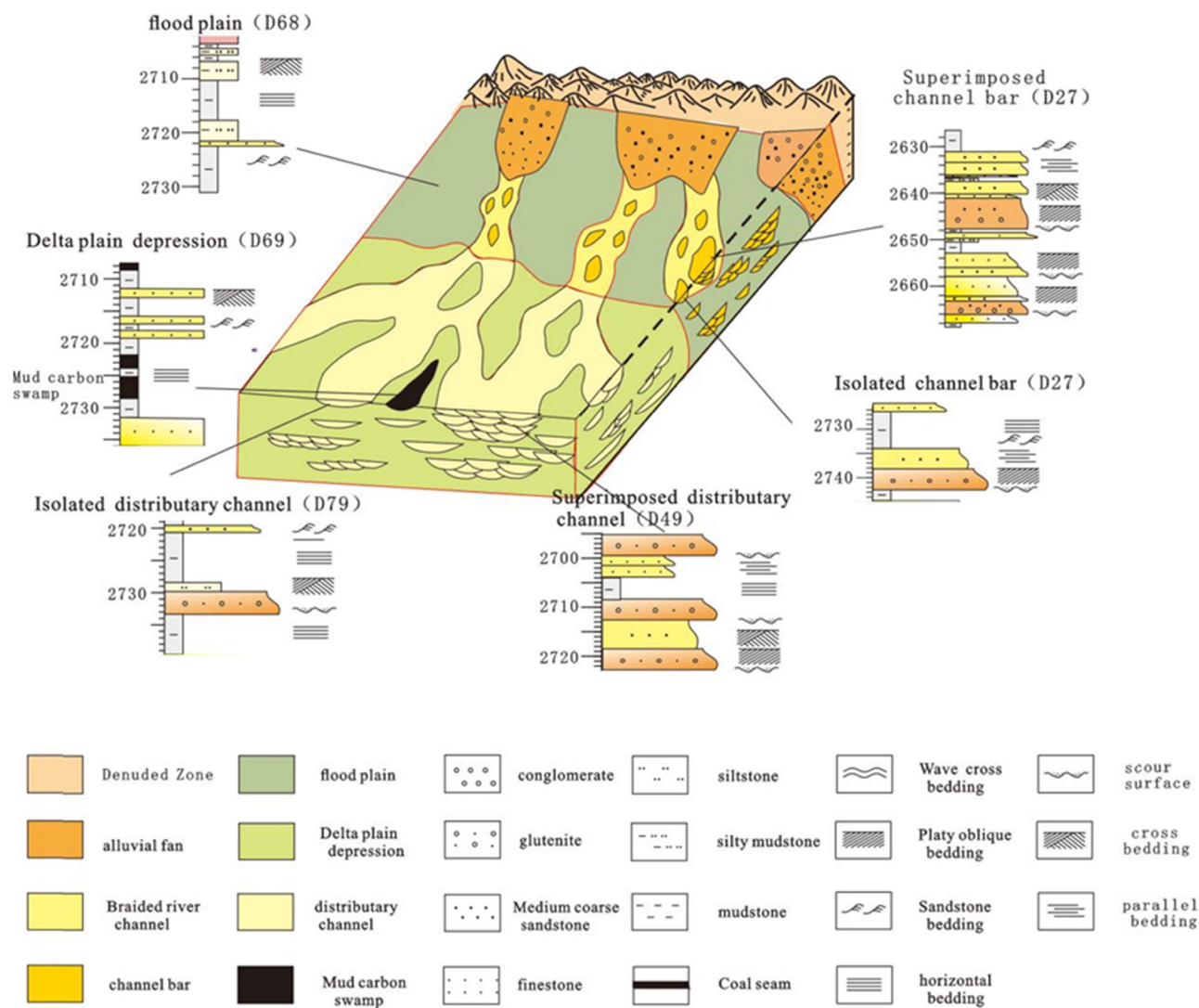


**Figure 7:** Distribution of porosity and permeability of Shanxi Formation in the study area.








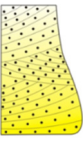

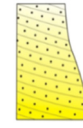



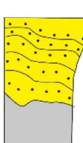

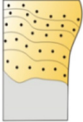

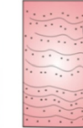




**Figure 8:** Distribution of porosity and permeability in the first member of the Lower Shihezi Formation in the study area.



**Figure 9:** Sedimentary model of Shanxi Formation and Lower Shihezi Formation in the study area.

**Table 1:** Lithofacies division and genetic interpretation of Shanxi Formation–Lower Shihezi Formation in the study area

Lithofacies types	Main lithologic type	Sedimentary tectonics		Genetic interpretation	Lithofacies types	Main lithologic type	Sedimentary tectonics		Genetic interpret
Massive bedding conglomerate facies	Conglomerate			River bed detention	Gravel-bearing coarse sandstone facies	Gravel coarse sandstone			Distributary channel
Trough cross-bedding sandstone facies	Medium-coarse sandstone			Barrier sand dam Channel filling	Tabular cross-bedding sandstone facies	Medium-fine sandstone			Underwater classified river channel
Parallel bedding sandstone facies	Fine sandstone			High flow water, shallow rapids	Deformed stratified sandstone facies	Powder-fine sandstone			Estuary dam
Wave bedding sandstone facies	Fine-siltstone			Flow operation	Sand grained bedding siltstone facies	Fine sandstone			Tidal flat deposit
Horizontal bedding siltstone facies	Siltstone			Floodplains, natural levees	Dark mudstone facies	Dark mudstone			Former delta mud
					Light-colored mudstone facies	Light colored mudstone			Swamp sediment
					Coal and carbonaceous mudstone phases	Coal, carbonaceous mudstone			Swamp sediment

strong hydrodynamic conditions, the channel bar sand body usually has the characteristics of coarser grain size. In the field profile observation, it can be found that the fine-grained sediments at the top of the braided river channel bar are often eroded by the later developed channel bar, forming a phenomenon of multiple channel bar superposition, which is closely related to the frequent diversion of the braided channel [57,58]. At the bottom of the channel bar, large trough cross-bedding and a small amount of ripple cross-bedding are developed. At the same time, the close distance to the source area and the short transportation distance result in a lower maturity of sand body composition and structure.

#### 4.3.2.1.2 Flood plain

The flood plain is mainly formed outside the braided river channels. The lithology is mudstone, siltstone, and a small amount of fine sandstone, and a large number of plants grow in the low-lying terrain, which is a powerful sedimentary environment for the formation of coal seams.

#### 4.3.2.2 Braided river delta

##### 4.3.2.2.1 Delta plain distributary channel

In the delta plain, distributary channels form the primary depositional environment, characterized by coarse-



grained sedimentation. After long-distance transportation, the sediments are well sorted and rounded, and the bottom of the sediment develops a scour filling structure. Distributary channel deposits have channel sedimentary characteristics, usually developed at the bottom of the large trough-shaped cross-bedding, and the channel sedimentary sequence is obvious.

#### 4.3.2.2.2 Interchannel deposition

Depression is the main sedimentary type of interchannel deposition, in a relatively low-lying area, developed between distributary channels. The sediments are mainly mudstone, in which horizontal bedding is occasionally seen. When a river channel breaks, a small amount of siltstone and fine sandstone are deposited in the depression. Swamps can be formed in depressions. The swamps are heavily vegetated, poorly drained, stagnant reductive environments, and are characterized by well-preserved plant fragments and abundant authigenic minerals such as pyrite.

## 5 Discussion

### 5.1 Sedimentation model

#### 5.1.1 Distributary channel development model

Based on the scale, lithological characteristics, and development location of the distributary channel, the main distributary channel and the secondary distributary channel are divided. The main distributary channel is characterized by multiple sets of gravelly coarse sandstone and coarse sandstone combinations on the profile. The sand bodies are coarse-grained and well connected in the lateral and vertical directions, and the lithofacies is mainly (gravelly) coarse sandstone. The sub-distributary river section shows a complete channel sedimentary sequence, and there is a mudstone interval between the upper and lower channel sand bodies.

The main distributary channel usually develops in the center of the river channel or at the intersection of distributary channels. Its development is affected by the accommodation space of the lake basin. When the level of the lake basin decreases, the accommodation space in the basin increases, and the sand body expands to the lake basin on a large scale, which promotes the extensive development of the distributary channels. In the area of intensive development of distributary channels, overlap phenomenon usually occurs between distributary channels,

forming main distributary channels. In the area with less distributary channel development, the developed mudstone deposits between distributary channels to form sub-distributary channel deposits.

#### 5.1.2 Channel bar development model

The channel bar is divided into high-energy channel bar sand body and low-energy channel bar. The high-energy channel bar is mainly composed of (gravelly) coarse sandstone lithofacies. The lithofacies of low energy channel bar is medium-coarse sandstone or medium-fine sandstone. Due to the short transportation distance, the particle sorting and roundness of these sand bodies are usually poor. The high-energy channel bar is characterized by multiple sets of sand bodies superimposed, the sedimentary sequence is incomplete, and the top fine-grained sediment is often replaced by coarse gravel sandstone at the bottom, and the sand body granularity is coarser. The low-energy channel bar is composed of a single sand body, its sedimentary sequence is complete, and the grain size gradually becomes finer upward. The high-energy channel bar is usually developed near the central axis of the channel sand body belt and in the local height difference area, and is distributed lenticular or banded.

### 5.2 Impacts on the reservoir

The influence of sedimentation on the reservoir can be observed in three aspects: clastic particle composition, lithology change, and sedimentary microfacies.

#### 5.2.1 Influence of clastic particle composition on the reservoir

The clastic particles are composed of quartz, feldspar, and debris. By analyzing the particle content and porosity data of typical wells in the study area, we found a negative correlation between quartz content and porosity of the reservoir (Figure 10a). Quartz particles are relatively stable, and a small amount of quartz particles is conducive to reducing compaction, which is beneficial to the reservoir [59]. However, when the quartz content is too high, it leads to a decrease in the content of feldspar and debris, which is not conducive to the dissolution of these particles in the later stage. Feldspar content is also negatively correlated with porosity (Figure 10b). The dissolution of feldspar particles can form intragranular and intergranular pores, which is beneficial to the reservoir. Thin section observation shows that the

samples with more feldspar particles dissolved usually have higher porosity, while the large number of intact feldspar particles without corrosion indicates insufficient corrosion. There is a positive correlation between debris content and porosity (Figure 10c). The debris particles are of different sizes and complex in composition, and can form large number of intergranular dissolved pores, which have a positive impact on the reservoir.

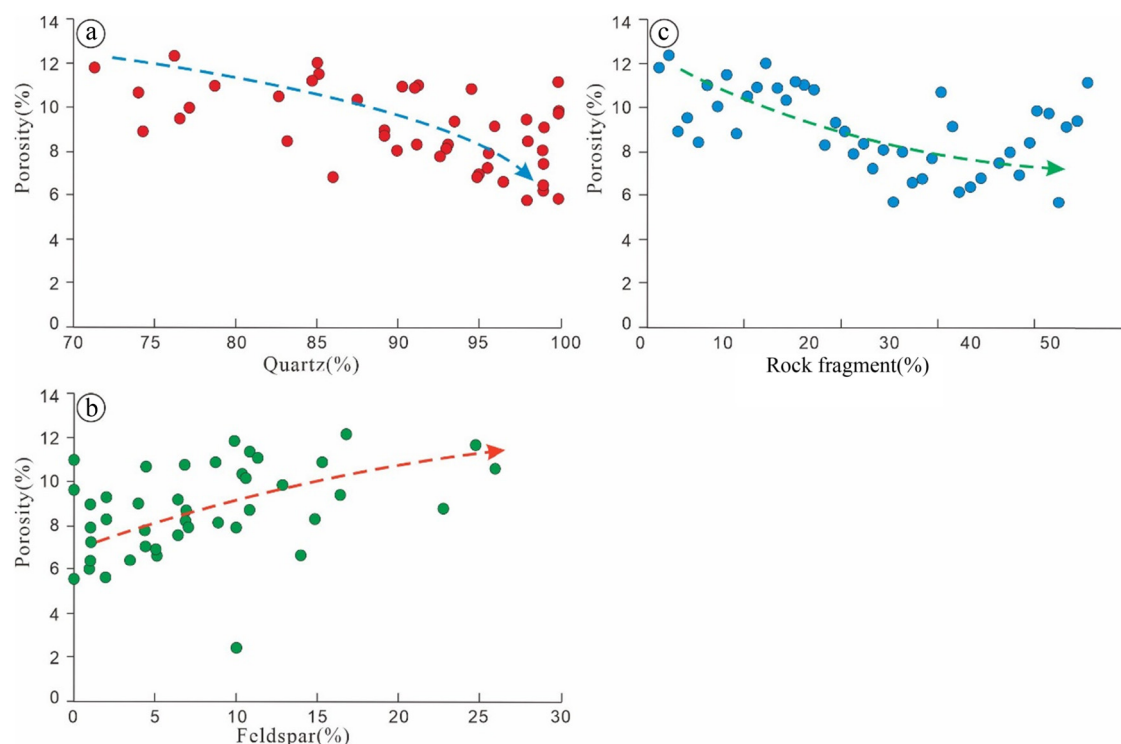
### 5.2.2 Influence of lithology on reservoir

By comparing the porosity of different rock types in the study area (Figure 11), we found that changes in gravel content have no significant effect on porosity of the reservoir. Whether it is gravelly coarse sandstone, coarse sandstone, gravelly medium sandstone, and medium sandstone, the porosity does not change much. The average porosity of pebbly fine sandstone (6.8%) is lower than that of fine sandstone (8.2%). According to the location of the well section selected for the sample, although the gravel-bearing part developed at the bottom of the river channel has a coarser grain size, due to insufficient thickness and large changes in lithology, the porosity of the reservoir changes greatly and the average porosity is not high. It is worth

noting that the fine sandstone and a small amount of medium sandstone developed in the middle of the river channel, although the plate bedding, trough bedding, and parallel bedding were developed and the thickness was large, the average porosity did not increase significantly. In general, the lithology of the reservoir in the study area changes frequently, and the impact on porosity is not significant.

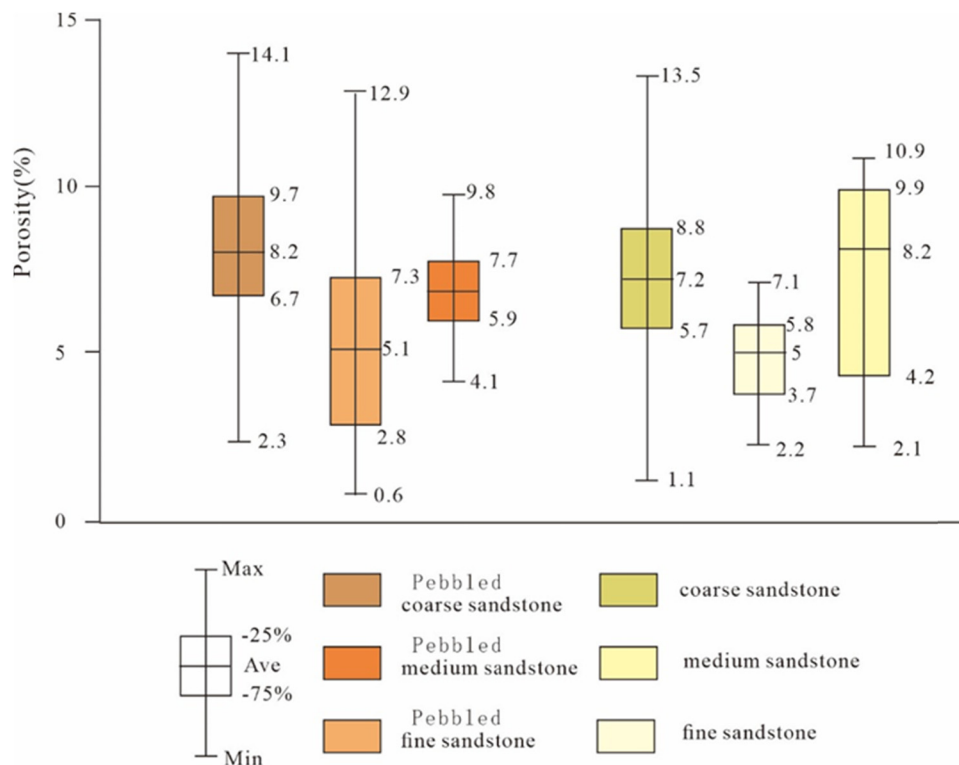
### 5.2.3 Influence of sedimentary microfacies on reservoirs

In the braided river sedimentary environment, we compared the isolated and superimposed channel bars (Figure 12). It is found that the porosity and permeability of the superimposed channel bar are significantly higher than that of the isolated channel bar, with the porosity range of superimposed channel bar being 8–15% and the permeability being  $0.3\text{--}2.2 \times 10^{-3} \text{ m}^2$ . The porosity of the isolated channel bar is 7–9%, and the permeability is  $0.4\text{--}1.2 \times 10^{-3} \text{ m}^2$ . In the delta plain, we compared the main distributary channel with the secondary distributary channel and found that the porosity of the main distributary channel is 8–13%, and the permeability is  $0.3\text{--}0.6 \times 10^{-3} \text{ m}^2$ , while the porosity of the secondary distributary channel is 7–11%, and the permeability is  $0.2\text{--}0.5 \times 10^{-3} \text{ m}^2$ . In summary, we believe that the porosity and permeability of the



**Figure 10:** Relationship between particle content and porosity of clastic reservoir in the study area: (a) relationship between quartz content and porosity, (b) relationship between debris content and porosity, and (c) relationship between feldspar content and porosity.





**Figure 11:** Porosity distribution of different rock types in Shanxi Formation–Lower Shihezi Formation first member in the study area.

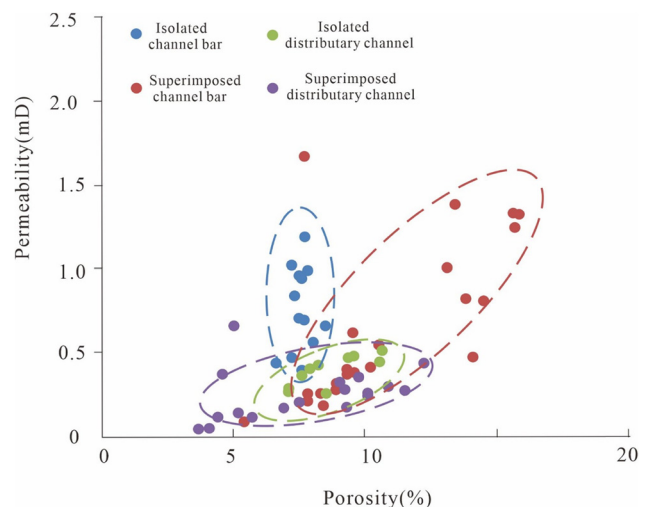
channel bar microfacies are generally better than those of the distributary channel microfacies, which may be closely related to the hydrodynamic conditions in the sedimentary environment.

In addition, in the braided river environment, the channel bar usually has an inconspicuous “binary structure” of sandstone and mudstone due to its overall coarse grain size, the development of conglomerate deposits at the bottom, and the inconspicuous fine-grained deposits at the top. The distributary channel deposits usually have a complete sedimentary sequence, and the grain size in the upper part gradually becomes finer, transitioning to the natural levee and floodplain sedimentary environment dominated by mudstone. It is worth noting that although the sedimentary sequence of the reconstructed overlapped channel bar and channel is incomplete, they lack fine sediment at the top, but possess good porosity and permeability, and large-scale sand bodies are conducive to the formation of high-quality reservoirs in the study area.

### 5.3 Sedimentary models favorable for oil and gas enrichment

Based on our comprehensive analysis, the main distributary channel in the delta sedimentary environment and the

high-energy channel bar in the braided river are two sedimentary models that are conducive to oil and gas enrichment, both formed under relatively high hydrodynamic conditions. The main distributary channel is usually developed in the center of the river or at the confluence of the diversion channels, and is mostly superposed, with



**Figure 12:** The physical characteristics of different sedimentary facies in Shanxi Formation–Lower Shihezi Formation first member in the study area.

porosity of 8–13% and permeability of 0.3–0.6 md. The high-energy channel bar is characterized by the superposition of multiple sets of sand bodies. The sedimentary sequence is not complete, with fine-grained sediments at the top usually replaced by pebbly coarse sandstone. The sand body has a coarse particle size, with porosity of 8–15% and permeability of 0.3–2.2 md. Therefore, we speculate that these two sedimentary models may be the focus of future oil and gas exploration and provide significant reference value for similar areas.

## 6 Conclusion

- (1) The first member of the Lower Shihezi Formation in the study area is mainly composed of lithic quartz sandstone and lithic sandstone, and only a few samples are classified as feldspar lithic sandstone. The Shanxi Formation is mainly composed of lithic quartz sandstone, lithic sandstone, quartz sandstone, and a small amount of feldspar lithic sandstone.
- (2) The pore types of clastic rocks in the study area mainly include intergranular dissolved pores, intragranular dissolved pores, and microfractures. The average porosity of the first member of Lower Shihezi Formation is 7.28%, and the average permeability is  $0.86 \times 10^{-3} \text{ m}^2$ . The average porosity of Shanxi Formation is 6%, and the average permeability is  $0.262 \times 10^{-3} \text{ m}^2$ .
- (3) The Shanxi Formation belongs to delta plain sediments, including distributary channel and interchannel deposits, which are divided into main distributary channel and secondary distributary channel microfacies. The first member of the Lower Shihezi Formation is a braided river deposit, including channel bar deposits and flood plain deposits, and isolated channel bar and superimposed channel bar microfacies are identified.
- (4) Sample analysis shows that sedimentation significantly affects reservoir physical properties through particle, lithology, and sedimentary microfacies characteristics. The main distributary channel and superimposed channel bar are favorable sedimentary microfacies for the formation of gas reservoirs. The porosity of the main distributary channel is 8–13%, and the permeability is  $0.3\text{--}0.6 \times 10^{-3} \text{ m}^2$ ; the porosity of the superimposed channel bar is 8–15%, and the permeability is  $0.3\text{--}2.2 \times 10^{-3} \text{ m}^2$ . This study provides a theoretical basis for the development of tight sandstone gas reservoirs in Daniudi gas field.

**Acknowledgments:** The authors gratefully acknowledge two anonymous reviewers and Analogue Modelling of Zunyi Normal College for their insightful suggestions.

**Funding information:** This work is funded by the Science and Technology innovation team of colleges and universities of Guizhou Education Department project “Research on Evaluation Methods of Shale gas blocks in Zunyi Area” (project number: [2024]207).

**Author contributions:** Chenyu Yang: conceptualization, data curation, formal analysis, investigation, methodology, resources, visualization, writing – original draft; Hang Yu: resources, investigation, validation, writing – review & editing; Hui Xie: conceptualization, supervision, validation, writing – review & editing; Shunfeng Peng: investigation, methodology, resources, writing – review & editing; Jiangfei Tian: methodology, validation, visualization, writing – review & editing; Zhiwu Gao: writing – review & editing; Chenyu Yang: writing – review & editing; Tian Luo: conceptualization, investigation, methodology, resources, validation, visualization, writing – review & editing.

**Conflict of interest:** The authors declare that the research was conducted in the absence of any commercial or financial relationships that could be construed as a potential conflict of interest.

**Data availability statement:** The datasets generated during and/or analysed during the current study are available from the corresponding author on reasonable request.

## References

- [1] Tylor TR, Giles MR, Hathon LA, Diggs TN, Braunsdorf NR, Birbiglia GV, et al. Sandstone diagenesis and reservoir quality prediction: models, myths, and reality. *AAPG Bull.* 2010;94(8):1093–132.
- [2] Bjørlykke K. Relationships between depositional environments, burial history and rock properties. Some principal aspects of diagenetic process in sedimentary basins. *Sediment Geol.* 2014;301:1–14.
- [3] Ketzer JM, Holz M, Morad S, Al-Aasm IS. Sequence stratigraphic distribution of diagenetic alterations in coal-bearing, paralic sandstones: evidence from the Rio Bonito Formation (early Permian), southern Brazil. *Sedimentology.* 2003;50(5):855–77.
- [4] Kordi M, Turner B, Salem AMK. Linking diagenesis to sequence stratigraphy in fluvial and shallow marine sandstones: evidence from the Cambrian–Ordovician lower sandstone unit in southwestern Sinai, Egypt. *Mar Pet Geol.* 2011;28(8):1554–71.
- [5] Lai J, Wang GW, Ran Y, Zhou ZL. Predictive distribution of high-quality reservoirs of tight gas sandstones by linking diagenesis to depositional facies: evidence from Xu-2 sandstones in the Penglai area of the central Sichuan basin, China. *J Nat Gas Sci Eng.* 2015;23:97–111.



- [6] Morad S, Al-Ramadan K, Ketzer JM, Ros LF. The impact of diagenesis on the heterogeneity of sandstone reservoirs: a review of the role of depositional facies and sequence stratigraphy. *AAPG Bull.* 2010;94(8):1267–309.
- [7] Rahman MJJ, Worden RH. Diagenesis and its impact on the reservoir quality of Miocene sandstones (Surma Group) from the Bengal Basin, Bangladesh. *Mar Pet Geol.* 2016;77:898–915.
- [8] Lai J, Wang GW, Fan ZY, Chen J, Wang SC, Zhou ZL, et al. Insight into the pore structure of tight sandstones using NMR and HPMT measurements. *Energy Fuels.* 2016;30:10200–14.
- [9] Yu Y, Lin LB, Zhai CB, Chen HD, Wang YN, Li YH, et al. Impacts of lithologic characteristics and diagenesis on reservoir quality of the 4th member of the Upper Triassic Xujiahe Formation tight gas sandstones in the western Sichuan Basin, southwest China. *Mar Pet Geol.* 2019;107:1–19.
- [10] Lin LB, Yu Y, Nan HL, Chen H. Petrologic and geochemical characteristics of carbonate cements in the Upper Triassic Xujiahe Formation tight gas sandstone, western Sichuan Basin, China. *AAPG Bull.* 2022;106(2):461–90.
- [11] Dai JX, Ni YY, Wu XQ. Tight gas in China and its significance in exploration and exploitation. *Pet Explor Dev.* 2012;39(3):57–264. doi: 10.11698/PED.2012.03.002.
- [12] Zhu XM, Pan R, Zhu SF, Wei W, Ye L. Research progress and core issues in tight reservoir exploration. *Earth Sci Front.* 2018;25(2):141–6 (in Chinese with English abstract). doi: 10.11698/DXQY.2018.02.019.
- [13] Zou CN, Yang Z, He DB, Wei YS, Li J, Jia AL, et al. Theory, technology and prospects of conventional and unconventional natural gas. *Pet Explor Dev.* 2018;45(4):575–87.
- [14] Wei GQ, Zhang FD, Li J, Yang S, Huang CY, She YQ, et al. New progress of tight sand gas accumulation theory and favorable exploration zones in China. *Nat Gas Geosci.* 2016;27(2):199–210. doi: 10.11764/j.issn.1672-1926.2016.02.0199.
- [15] Sun LD, Zou CN, Jia AL, Wei YS, Zhu RK, Wu SK, et al. Development characteristics and orientation of tight oil and gas in China. *Pet Explor Dev.* 2019;46(6):1015–26. doi: 10.11698/PED.2019.06.01.
- [16] Zou CN, Yang Z, Zhu RK, Zhang GS, Hou LH, Wu ST, et al. Progress in China's unconventional oil & gas exploration and development and theoretical technologies. *Acta Geol Sin.* 2015;89(6):979–1007. doi: 10.11698/DZXE.2015.06.001.
- [17] Jia AL, Wei YS, Guo Z, Wang GT, Meng DW, Huang SQ. Development status and prospect of tight sandstone gas in China. *Nat Gas Ind.* 2022;42(1):83–92.
- [18] Wei XS, Hu AP, Zhao HT, Kang R, Shi XY, Liu XP. New geological understanding of tight sandstone gas. *Lithologic Reserv.* 2017;29(1):11–20. doi: 10.3969/j.issn.1673-8926.2017.01.002.
- [19] Zou CN, Tao SZ, Hou LH. *Unconventional oil and gas geology.* Beijing: Geological Publishing House; 2011. p. 1–92.
- [20] Zou CN, Zhang GS, Yang Z, Tao SZ, Hou LZ, Zhu RK, et al. Geological concepts, characteristics, resource potential and key techniques of unconventional hydrocarbon: on unconventional petroleum geology. *Pet Explor Dev.* 2013;40(4):385–99. doi: 10.11698/PED.2013.04.01.
- [21] Hao SM, Chen ZY, Li L. *The accumulation theory and practice of tight sandstone gas in Daniudi Gas Field, Ordos Basin.* Beijing: Petroleum Industry Press; 2011.
- [22] Wan YL, Li ZD, Peng C, Kong W, Xie YX, Zheng T. Reservoir characteristics and evaluation of low porosity and permeability sandstone of member of Shanxi Formation in Daniudi Gas Field, Ordos Basin. *Mineral Petrol.* 2016;36(3):106–14. doi: 10.19719/j.cnki.1001-6872.2016.03.01.
- [23] Qiu LW, Mu XJ, Li H, Zhang J, Ge J, Xu S, et al. Characteristics of detritus development in the Permian Lower Shihezi Formation in Hangjinqi area and its influence on reservoir physical properties. *Oil Gas Geol.* 2019;40(1):24–33. doi: 10.11743/ogg20190103.
- [24] Li YL, Jia AL, He DB. Control factors on the formation of effective reservoirs in tight sands: examples from Guang'an and Sulige gas fields. *Acta Petrolei Sin.* 2013;34(1):71–82. doi: 10.7623/syxb201301008.
- [25] Yu XH, Li SL, Yang ZH. Discussion on deposition-diagenesis genetic mechanism and hot issues of tight sandstone gas reservoir. *Lithologic Reserv.* 2015;27(1):1–13. doi: 10.3969/j.issn.1001-6872.2015-01-002.
- [26] Tian JC, Liang QS, Wang F, Yu W. Genesis and development model of tight oil reservoir sand body in continental lacustrine basin: a case study on the Upper Triassic Chang 6 pay zone, Ordos Basin. *Oil Gas Geol.* 2022;43(4):877–88. doi: 10.11743/ogg20220411.
- [27] Sun X, Wang J, Tao C, Zhang Y, Jia HC, Jiang HJ, et al. Evaluation of geochemical characteristics and source of natural gas in Lower Paleozoic, Daniudi area, Ordos Basin. *Pet Geol Exp.* 2021;43(2):307–14. doi: 10.11781/sysyd202102307.
- [28] Liu SL, Li H, Zhou XY. Relationship between sedimentary microfacies and reservoir productivity in Da12-Da66 well block, Daniudi gas field. *Oil Gas Geol.* 2012;33(1):45–9.
- [29] Dongshan YU, Guoqiang LI, Guichu MO. Evaluation of the Upper Paleozoic source rocks in the Daniudi Gas Field, Ordos Basin. *J Yangtze Univ (Nat Sci Ed) Sci Eng.* 2012;9(11):84–7. doi: 10.3969/j.issn.1673-1409(N).2012.11.028.
- [30] Liu Q, Jin Z, Meng Q, Wu X, Jia H. Genetic types of natural gas and filling patterns in Daniudi Gas Field, Ordos Basin, China. *J Asian Earth Sci.* 2015;107:1–11.
- [31] Yang Z, He S, Zou CN, Li QY, Chen ZY. Coupling relationship between reservoir diagenesis and natural gas accumulation of Daniudi gas field in north Ordos Basin. *Acta Petrolei Sin.* 2010;31(3):373–8. doi: 10.7623/syxb201003004.
- [32] Zheng WB, Hu XY, Chen SW, Liu JD, Jia C. Characteristics of sedimentary evolution in the Upper Paleozoic, Daniudi Gasfield, Ordos Basin. *Acta Sedimentol Sin.* 2015;33(2):306–13. doi: 10.14027/j.cnki.cjxb.2015.02.010.
- [33] Xu NN, Zhang SP, Wang YS, Qiu LW. Diagenesis and pore formation of the Upper Paleozoic tight sandstone in the northern area of the Ordos Basin. *Acta Sedimentol Sin.* 2022;40(2):422–34. doi: 10.14027/j.issn.1000-0550.2021.027.
- [34] Lei T, Wang Q, Ren GL, Zhu CB, Wang RY, Wang J, et al. Component characteristics of Shanxi Formation tight sandstone and their implications for the reservoirs in Ordos Basin: taking the A block of Daniudi Gas Field as an example. *Nat Gas Geosci.* 2023;34(3):418–30. doi: 10.11764/j.issn.1672-1926.2022.12.012.
- [35] Luo JL, Liu XS, Fu XY, Li M, Kang R, Jia YN. Impact of petrologic components and their diagenetic evolution on tight sandstone reservoir quality and gas yield: a case study from He 8 gas bearing reservoir of Upper Paleozoic in northern Ordos Basin. *Earth Sci: J China Univ Geosci.* 2014;39(5):537–45. doi: 10.3799/dqkx.2014.051.
- [36] Li S, Liu L, Wu J, Wang LL, Zhang ZL. Diagenetic evolution of tight sandstone of Shanxi-Lower Shihezi Formations in the southern Ordos Basin. *Nat Gas Geosci.* 2021;32(1):47–56. doi: 10.11764/j.issn.1672-1926.2020.09.008.
- [37] Xu NN, Wang YS, Zhang SP, Qiu LW, Zhang XJ, Lin R. Reservoir characteristics and diagenetic traps of the first member of Permian

- Xiashihezi Formation in Daniudi Gas Field, Ordos Basin. *Lithologic Reserv.* 2021;33(4):52–62. doi: 10.12108/xyq.20210406.
- [38] Gibling MR. Width and thickness of fluvial channel bodies and valley fills in the geological record: a literature compilation and classification. *J Sediment Res.* 2006;76:731–70. doi: 10.2110/jsr.2006.060.
- [39] Tan CP, Yu XH, Li SL, Li SL, Chen BT, Shan X, et al. Discussion on the model of braided river transform to meandering river: as an example of Toutunhe formation in southern Junggar Basin. *Acta Sedimentol Sin.* 2014;32(3):450–8. doi: 10.14027/j.cnki.cjxb.2014.03.009.
- [40] Jin ZK, Yang YX, Shang JL, Wang LS. Sandbody architecture and quantitative parameters of single channel sandbodies of braided river: cases from outcrops of braided river in Fukang, Liulin and Yanan area. *Nat Gas Geosci.* 2014;25(3):311–7. doi: 10.11764/j.issn.1672-1926.2014.03.0311.
- [41] Li SL, Yu XH, Chen BT, Li SL. Quantitative characterization of architecture elements and their response to base-level change in a sandy braided fluvial system at a mountain front. *J Sediment Res.* 2015;85(10):1258–74. doi: 10.2110/jsr.2015.82.
- [42] Li SL, Yu XH, Jiang T, Liang XR, Su DX. Meander-braided transition features and abandoned channel patterns in fluvial environment. *Acta Sedimentol Sin.* 2017;35(1):1–9. doi: 10.14027/j.cnki.cjxb.2017.01.001.
- [43] Wang M, Mu LX, Zhao GL, Wang YX. Architecture analysis of reservoirs in branching-and wandering-based braided rivers: taking FN field, Sudan as an example. *Earth Sci Front.* 2017;24(2):246–56. doi: 10.13745/j.esf.yx.2016-12-26.
- [44] Best JL, Ashworth PJ, Bristow CS, Roden J. Three-dimensional sedimentary architecture of a large, mid-channel sand braid bar, Jamuna River, Bangladesh. *J Sediment Res.* 2003;73(4):516–30. doi: 10.1306/010603730516.
- [45] Yu XH, Ma XX, Mu LX, Jia AL. Geological model and hierarchical interface analysis of braided river reservoir. Beijing: Petroleum Industry Press; 2004. p. 1–207.
- [46] Li W, Yue DL, Li J, Liu RJ, Guo CC, Wang WF, et al. Variable architecture models of fluvial reservoir controlled by base-level cycle: a case study of Jurassic outcrop in Datong basin. *Earth Sci.* 2022;47(11):3977–88. doi: 10.3799/dqkx.2022.132.
- [47] Li SL, Ma SP, Zhou LW, Huang XD, Han B, Li H. Main influencing factors of braided-meander transition and coexistence characteristics and implications of ancient fluvial sedimentary environment reconstruction. *Earth Sci.* 2022;47(11):3960–76. doi: 10.3799/dqkx.2022.013.
- [48] Li ZH, Huang WH. Lithofacies characteristics and sedimentary model of braided delta: a case study of He 8 member in the southern Sulige, Ordos Basin. *Lithologic Reserv.* 2017;29(1):43–50. doi: 10.3969/j.issn.1673-8926.2017.01.006.
- [49] Xu Z, Shen CS, Chen YK, Kang K, Luo XB, He XR, et al. Architecture characterization for sandy braided river reservoir and controlling factors of remaining oil distribution: a case study of Poilfield (Neogene), Bohai offshore, China. *Acta Sedimentol Sin.* 2016;34(2):375–85. doi: 10.14027/j.cnki.cjxb.2016.02.016.
- [50] Liu YM, Hou JG, Song BQ, Zhou XM, Chen HK, Zhang LM. Characterization of interlayers within braided-river thick sandstones: a case study on the Lamadian Oilfield in Daqing. *Acta Petrolei Sin.* 2011;32(5):836–41. doi: 10.7623/syxb201105015.
- [51] Sun TJ, Mu LX, Wu XH, Zhao GL, Xu F, Wang ZJ, et al. A quantitative method for architectural characterization of sandy braided-river reservoirs: taking Hegli oilfield of Muglad Basin in Sudan as an example. *Acta Petrolei Sin.* 2014;35(4):715–24. doi: 10.7623/syxb201404012.
- [52] Zhong DK. Micro-petrology, pore throat characteristics and genetic mechanism of tight oil reservoirs: a case from the 6th and 7th members of Triassic Yanchang Formation in the Ordos Basin. *Oil Gas Geol.* 2017;38(1):49–61. doi: 10.11743/ogg20170106.
- [53] Hao SM, Hui KY, Li L. Reservoiring features of Daniudi low-permeability gas field in Ordos Basin and its exploration and development technologies. *Oil Gas Geol.* 2006;27(6):762–8. doi: 10.11743/ogg20060606.
- [54] He FQ, Qi R, Wang FB, Deng J, Cheng L, Hu TL. Tectonic genesis of Triassic Yanchang Formation valley systems, southern Ordos Basin. *Oil Gas Geol.* 2021;42(5):1056–62. doi: 10.11743/ogg20210504.
- [55] Ma DY, Chen YH, Zhao JZ, Wu WT, Song P, Chen MN. Architectural elements of fluvial sand bodies of the eighth member of Permian Xiashihezi Formation in eastern Ordos Basin. *Lithologic Reserv.* 2023;5(1):63–73. doi: 10.12108/xyq.20230106.
- [56] Folk RL. Petrology of sedimentary rocks. Austin, TX: Hemphill; 1968. p. 107.
- [57] Qu XJ, Li JQ, Zhang J, Zhao Z, Qi ZL, Luo C. Quantitative characterization of reservoir architecture units of braided river tight sandstone reservoirs. *J Jilin Univ (Earth Sci Ed).* 2018;48(5):1342–52. doi: 10.13278/j.cnki.jjuese.20170155.
- [58] Yu CL, Li ZP, Xiong YB, Wu S, Zeng P. Analysis on internal architecture of batture bar reservoir. *J Southwest Pet Univ (Sci Technol Ed).* 2012;34(3):19–23. doi: 10.3863/j.issn.1674-5086.2012.03.003.
- [59] Yang XP, Zhao WZ, Zou CN, Chen MJ, Guo YR. Origin of low-permeability reservoir and distribution of favorable reservoir. *Acta Petrolei Sin.* 2007;28(4):57–61. doi: 10.3321/j.issn:0253-2697.2007.04.011.